NEOPLASMA accepted, ahead of print manuscript
Cite article as https://doi.org/10.4149/neo_2026_251105N462

Running title: SMAP1 promotes hepatoblastoma cell proliferation

SMAP1 promotes hepatoblastoma cell proliferation by modulating the C-Kit-activated ERK/MAPK pathway

Jie Liu[1,2,#,*], Ke Xu[3,#], Hongyue Wang[3,#], Yan Cheng[3], Zihui Cheng[3], Wenjie Bu[2], Feifei Wang[4,5], Xiaoxuan Zuo[6], Xiaojian Li[7], Nan Xia[4,5,8], Qian Dong[4], Wenli Xiu[4], Aiqin Lin[2,*]

[1]Department of Pediatric Surgery, The First Affiliated Hospital of Wannan Medical University (Yijishan Hospital of Wannan Medical University), Wannan Medical University, Wuhu, China; [2]Department of Medical Biology of Wannan Medical University, Wannan Medical University, Wuhu, China; [3]Department of Clinical Medicine of Wannan Medical University, Wannan Medical University , Wuhu, China; [4]Department of Pediatric Surgery, Affiliated Hospital of Qingdao University, Qingdao University, Qingdao, China; [5]Shandong Provincial Key Laboratory of Digital Medicine and Computer-assisted Surgery, Affiliated Hospital of Qingdao University, Qingdao, China; [6]Department of Youth League Committee, Wannan Medical University, Wuhu, China; [7]The Third Department of Gastrointestinal Surgery, Yijishan Hospital of Wannan Medical University, Wannan Medical University, Wuhu, China; [8]Institute of Digital Medicine and Computer-assisted Surgery of Qingdao University, Qingdao University, Qingdao, China

*Correspondence: linaiqin945@163.com; liujie19842020@163.com

[#]Contributed equally to this work.

Received November 5, 2025 / Accepted July 9, 2026

Hepatoblastoma (HB) is the most common pediatric liver malignancy. We investigated the role of SMAP1 in HB proliferation and its mechanism. Sixty-seven HB tissues were analyzed for SMAP1 expression via immunohistochemistry and correlated with clinical outcomes. qRT-PCR quantified SMAP1 mRNA in HB cell lines versus normal hepatocytes. SMAP1 was knocked down (siRNA/lentivirus) or overexpressed (plasmid) in HB cells; proliferation was assessed by CCK-8 and colony formation. A nude-mouse xenograft model was used to evaluate tumorigenicity. Western blotting determined C-Kit and ERK/MAPK pathway activity after SMAP1 modulation. Rescue experiments used ERK activator C16-PAF, inhibitor U0126, or C-Kit inhibitor ISCK03. SMAP1 was upregulated in HB and predicted poor prognosis. Knockdown reduced C-Kit, p-C-Kit, and p-ERK1/2, inhibited proliferation and colony formation, and suppressed xenograft growth. Overexpression produced opposite effects. U0126 reversed ERK1/2 phosphorylation and p-Rb in SMAP1-overexpressing cells, whereas C16-PAF restored ERK signaling and c-Myc/p-Rb in knockdown cells. ISCK03 blocked C-Kit/ERK activation prompted by SMAP1 overexpression. SMAP1 drives HB progression by activating C-Kit-ERK/MAPK signaling, representing a potential therapeutic target.

Key words: hepatoblastoma; SMAP1; C-Kit; ERK/MAPK

Hepatoblastoma (HB) is the most common malignant tumor of the liver in children. Although the incidence of HB is approximately 1.5 cases per one million children, the pathogenesis of the disease remains unclear [1]. Although the combination of neoadjuvant chemotherapy and surgery has greatly improved patient outcomes, the 5-year survival rate for patients with PRETEXT stage III/IV disease remains low [2-4]. Therefore, the precise diagnosis and treatment of childhood HB and the development of novel therapeutic strategies are urgent challenges [5]. To achieve these goals, a better understanding of the molecular mechanisms underlying the occurrence and development of HB is necessary.

Through exome sequencing, our previous research revealed that the *SMAP1* gene exhibits high-frequency copy number variations in HB [6]. The SMAP1 gene is located at chr6q13, spanning 11 exons with a total length of 194,132 bp. SMAP1 encodes a 467-amino-acid protein that includes an Arf-GAP domain, a C4-type zinc finger, and clathrin- and CALM-binding motifs [7]. SMAP1 binds the clathrin heavy chain and regulates clathrin-dependent endocytosis of the transferrin receptor and E-cadherin. Although *SMAP1* mutations have been linked to several diseases [8-10], its role in HB has not been described. According to literature reports, C-Kit, also known as Kit or CD117, is a receptor for stem cell factor (SCF) and a protein that is frequently overexpressed in gastrointestinal stromal tumors, small cell lung cancer, hepatocellular carcinoma, and leukemia, and is closely associated with tumor development [11, 12]. Notably, hepatoblastoma cells have been shown to secrete stem cell factor (SCF), the ligand of C-Kit, supporting a paracrine role for this receptor in the hepatic microenvironment [11]. Moreover, C-Kit participates in the MAPK, PI3K, and JNK/SAPK cascades; the small GTPase Ras activates the MAPK cascade by promoting the phosphorylation of various transcription factors, after which activated extracellular signal-regulated kinase (ERK) translocates to the nucleus to regulate gene expression [13, 14]. The ERK/MAPK pathway, the first MAPK subfamily identified, transmits extracellular stimuli to intracellular targets through sequential phosphorylation thereby modulating cell survival, proliferation, differentiation, and invasion and is closely associated with tumorigenesis, progression, metastasis, and therapeutic response [15]. Building upon our previous research, the present study investigated whether *SMAP1* regulates cell proliferation and the related molecular mechanisms in HB by modulating the C-Kit-activated ERK/MAPK signaling pathway.

Patients and Methods

Tissue collection. Tumor tissue and adjacent tissue samples of pediatric HB patients who underwent surgical treatment were collected from the clinical sample banks of Qingdao University Affiliated Hospital and Yijishan Hospital of Wannan Medical University from February 2000 to February 2025. The patient inclusion criteria were as follows: 1) first pathological diagnosis of HB; and 2) available detailed clinical data and basic personal information. The exclusion criteria were as follows: 1) the presence of other cancers and 2) no detailed follow-up data available. Immunohistochemical staining was performed on the HB tumor tissue and adjacent normal liver tissue according to a previously reported method [16], according to which the expression of the SMAP1 protein was detected and scored. The staining score was determined according to the percentage of positively stained cells (0=less than 5%, 1=5-25%, 2=26-50%, 3=51-75%, and 4=more than 75%) and the intensity of staining (0-3). The total score was obtained by multiplying the percentage score by the intensity score [6]. All tissue samples were obtained with the consent of the patient's family members, who signed informed consent forms. The present study was approved by the Ethics Committee of Qingdao University Affiliated Hospital (Approval No.: QYFY WZLL 25776) and the Medical Ethics Committee of Wannan Medical University (Approval No.: LLSC-2022-16). The median IHC score of SMAP1 was used as the cut-off value to stratify patients into high-expression and low-expression groups. The cut-off value was set at 5, the median score of all 67 cases. Patients with a score ≥ 5 were assigned to the SMAP1 high-expression group, and those with a score < 5 were assigned to the low-expression group.

Cell culture. HuH-6 cells (#CC0114, CellCook) were cultured in modified DMEM medium (CM2007, CellCook) supplemented with 10% fetal bovine serum (#S711-001S, Lonsera), Hep-G2 cells (#CC0101, CellCook) were cultured in MEM medium (#SH30024, HyClone) supplemented with 10% fetal bovine serum, and THLE-2 cells (#SC0659, Yuchicell) were cultured in THLE-2 Cell-specific culture medium (#CX0123, Yuchicell). The cell lines were cultured at 37 °C in the presence of 5% carbon dioxide. When the cell density reached 80-90%, the cells were digested with 0.25% trypsin (#25200056, Gibco) and placed in a six-well plate for subculture.

siRNA transfection. The st-h-*SMAP1* (si-*SMAP1*) and siRNA-negative control (si-NC) were constructed by RiboBio biotechnology Company, Guangzhou. The sequences are shown in Table 1.

When the cell density in the six-well plate reached 30-50%, the culture medium was replaced with fresh complete culture medium. si-*SMAP1* (20 μM) and si-NC (20 μM) were transfected into the cells using transfection reagents (#C10511-05, Ribobio) in two wells each according to the manufacturer's instructions; non-transfected cells in the other two wells served as blank controls. RNA was extracted 24 h after transfection, and total protein was extracted 48 h after transfection. The transfection efficiency was determined by RT-qPCR and Western blot assays.

Plasmid transfection. The *SMAP1* overexpression plasmid (OE-*SMAP1*) and its control empty plasmid (OE-NC) were constructed by RiboBio biotechnology Company, Guangzhou. The sequences are detailed in the Supplementary Table S1. When the cell density in the six-well plate reached 80-90%, the culture medium was replaced with fresh complete culture medium. The OE-*SMAP1* (1 μg) and OE-NC (1 μg) were transfected into the cells using transfection reagents (#SL100568, GenMute) in two wells each according to the manufacturer's instructions; non-transfected cells in the other two wells served as blank controls. RNA was extracted 24 h after transfection, and total protein was extracted 48 h after transfection. The transfection efficiency was determined by RT-qPCR and Western blot assays.

RNA extraction and qRT-PCR. Total RNA was extracted from the cells using TRIzol reagent (#15596026, Invitrogen), and the RNA concentration and purity were determined using a micro nucleic acid protein analyzer. First, the RNA concentration was adjusted uniformly to 0.5 μg/ml. RNA was reverse transcribed into cDNA using a reverse transcription kit (#M1701, Promega), and relevant genes were amplified by fluorescence quantitative PCR using ACTB as an internal reference. The $2^{-\Delta\Delta ct}$ method was used to quantify gene expression. The sequences of the primers are shown in Table 2.

Protein extraction and western blot analysis. The cells were lysed with Western and IP lysis buffer (#P0013, Beyotime) on ice for 10 min, followed by centrifugation at 4 °C and 13,000 × g for 10 min. The total cell protein was then extracted, and the protein concentration was measured using BCA kit (#P0012, Beyotime) and adjusted to be consistent in each group (10 μg/μl). SDS-PAGE protein loading buffer (5×) (#P0015, Beyotime) was added to the samples, after which they were denatured in a metal bath at 100 °C for 10 min. The samples were stored at -20 °C until further use. Protein samples (5 μl) were separated by SDS-PAGE, then transferred onto Nitrocellulose membranes (#HATF00010, Immobilon-NC) using the wet transfer method. The membranes were blocked with TBST containing 5% skim milk powder (#BR010A, Biomiky) for 2 h. After washing,

the membranes were incubated with the primary antibodies overnight at 4 °C. The membranes were then washed three times with TBST and incubated with the secondary antibodies. After washing the membranes three times, the protein bands were detected using ECL luminous solution (#BMU102, SuperKine) and a fluorescence and chemiluminescence gel imaging system (FluorChem E, ProteinSimple, USA). The experimental results were analyzed using the AlphaView SA software. The relevant antibody information is as follows: SMAP1 (#P103787, Yamei), p44/42 MAPK (Erk1/2) (#4695T, CST), Phospho-p44/42 MAPK (#4370T, CST), c-Kit (#3074T, CST), Phospho-c-Kit (Tyr703) (#3073T, CST), GAPDH (#AF1186, Beyotime), c-Myc (c-Myc, CST), and Phospho-Rb (#8516S, CST). HRP-labeled secondary antibody (#A0208, #A0216, Beyotime).

CCK-8 proliferation assay. After the cells were transfected with the siRNA, overexpression plasmid or respective control for 24 h, they were digested with 0.25% trypsin. A cell counter (Celldrop BF, Denovix) was used to obtain a cell suspension of 50,000 cells/ml. Cell suspension, PBS, or cell culture medium (100 µl/well) was added to a each well in a 96 well plate (6 replicates/group), which was then incubated. After treatment, the cells were incubated with 10% CCK8 reagent (#MK001B, Biomiky) every 24 h until 72 h at 37 °C for 1-2 h. Finally, the absorbance of each well was measured at a wavelength of 450 nm using a microplate reader (SYNERGY H1, BioTek) and analyzed.

Colony-formation assay. After the cells were transfected with the siRNA, overexpression plasmid or respective control for 24 h, they were digested with 0.25% trypsin. A cell counter was used to dilute the cell suspension to 500 cells/ml. In a new six-well plate, 2 ml of diluted cell suspension was added according to the original grouping, with 6 replicates per group. The cells were observed every 24 h, and the culture medium was replaced regularly for one week. At the end of this period, when visible colonies had formed, the cells were fixed with methanol (1.5 ml) for 30 min. After the methanol treatment, the sample was washed twice with PBS, then stained with crystal violet staining solution (#C0121, Beyotime) at room temperature for 15 min, and finally rinsed with clean water slowly until the background became clear. The cell colonies were imaged under the 4× eyepiece to count the number of colonies.

Xenotransplantation model for subcutaneous tumor formation in nude mice. Ten 5-week-old female BALB/c nude mice were obtained from Qinglongshan Experimental Animal Center (Nanjing, China) and isolated in the SPF animal room for 3 days. The mice were randomly divided into the following two groups, with 5 mice in each group: the stable *SMAP1* knockdown group (KD)

and the NC group (NC). The mice were given sterile water, food, and bedding. Stably transformed *SMAP1* knockdown and NC HuH-6 cells were seeded into a 10 cm culture dish and allowed to grow logarithmically until a cell density of 80-90% was reached. The cells were digested and centrifuged, and the supernatant was discarded. The cells were resuspended in PBS (5×10^7 cells/ml) subcutaneously inoculated into the mice at a dose of 0.1 ml. The health, behavior and weights of the animals were recorded every three days. Starting from the second week, the subcutaneous tumor size was measured. The tumor volume was calculated using the following formula: tumor volume=length × width²/2. At 3 weeks post-inoculation, the mice (n=10) were anesthetized with 5% isoflurane and euthanized within 5 minutes by cervical dislocation. Before subjected to euthanasia, the survival rate of the mice was 100%. All animals were fully anesthetized before euthanasia: each mouse was placed in a sealed induction chamber and exposed to 5 % isoflurane in 100 % O_2 at a flow rate of 1 L min^{-1} until loss of the righting reflex (achieved within ≤ 60 s). After confirming deep anesthesia (absence of toe-pinch and corneal reflexes), mice were immediately removed from the chamber and euthanized by cervical dislocation within 5 min of the initial anesthetic exposure. This sequence ensures the animals were completely unconscious and insensitive to pain at the moment of sacrifice. The protocol follows the 2020 AVMA Guidelines for the Euthanasia of Animals (accepted method: "inhaled anesthetic followed by cervical dislocation") and was approved by the Animal Ethics Committee of Wannan Medical University (Approval No. LLSC-2022-065). The dissected tumors were weighed, and a portion of each tumor was fixed with 4% paraformaldehyde solution for subsequent immunohistochemical experiments. All the experimental procedures were conducted in accordance with international guidelines.

Immunohistochemistry for Ki-67 and cleaved caspase-3. The paraffin-embedded tumor tissue sections from the nude mice were routinely deparaffinized and immersed in different concentrations of alcohol (100% → 90% → 80% → 70% → 50%, 3 min each), and they were then rinsed with distilled water for 3 min. After treatment with citrate buffer (pH=6.0), the sections were subjected to an antigen retrieval process using a microwave. The sections were then washed three times with PBS (3 min each) and blocked with 5% goat serum at 36 °C for 1 h. The sections were incubated with Ki-67 antibody (#GB111141, Servicebio, China; 1:500) and caspase-3 antibody (#19677-1-AP, Proteintech, USA; 1:300) overnight at 4 °C. After washing the sections 3 times with PBS (3 min each), they were incubated with human rabbit secondary antibodies at 37 °C for 1 h. The sections were then washed 3 times with PBS (3 min each time), stained with DAB for 5 s, counterstained

with hematoxylin for 30 s, washed with tap water for 3 min, dehydrated with different concentrations of alcohol (50% → 70% → 80% → 90% → 100%, each time for 3 min), air dried, cleared with xylene for 5 min, and sealed. The corresponding scan results were observed and saved on an immunohistochemical scanner. Ki-67-positive staining was indicated by brown staining in the nucleus, while capase-3-positive staining was indicated by brown staining in the cytoplasm. The expression of Ki-67 and caspase-3 was evaluated by combining the comprehensive score of the staining intensity and staining area. The IHC scoring criteria were the same as those above.

***In vivo* bioluminescence imaging.** The nude mice were weighed before the experiment, and the tumor size was measured. At 10-15 min before imaging, fluorescent dye stock solution (15 mg/ml, #HY-12591B, MCE) was injected into the abdominal cavity according to the weight of the nude mouse (final concentration 150 mg/kg), D-Luciferin was used as the substrate for *in vivo* bioluminescence imaging. Approximately 5 min before imaging, the nude mouse was anesthetized with 5% isoflurane. The tumor of the nude mouse was placed facing upward, and pictures were acquired in a uniform position using the small animal live imaging device (IVIS Lumina LT, PE Company, USA). The mouse was then returned to the cage, and the status of the nude mouse was observed until autonomous activity was resumed.

ERK/MAPK pathway rescue experiments. After the cells were transfected with si-*SMAP1* or NC for 24 h, they were treated with the ERK activator C16-PAF (#HY-108635, MCE, at a final concentration of 1 μM) for 24 h, and total protein was extracted. Two hours before transfection with the *SMAP1* overexpression plasmid or NC plasmid, the cells were treated with the ERK inhibitor U0126 (#HY-12031, MCE, at a final concentration of 10 μM) was added. After 48 h of treatment, total protein was extracted, and changes in the expression of related proteins after the addition of an ERK activator and inhibitor were detected by Western blot analysis.

C-Kit interference assay. After the cells were transfected with the *SMAP1* overexpression plasmid or NC plasmid for 12 h, they were treated with the C-Kit inhibitor ISCK03 (#HY-101443, MCE, at a final concentration of 10 μM) for 48 h, and total protein was extracted. The changes in the expression of related proteins after the addition of a C-Kit inhibitor were detected by Western blot analysis.

Statistical analysis. SPSS 26.0 and R 4.2.0 were used to analyze the data. The normality of the data was assessed using the Shapiro-Wilk test. Categorical variables were compared using chi-square tests or Fisher's exact tests when appropriate. Continuous variables were compared using Student's t

tests or Mann-Whitney U tests, depending on the distribution of the data. The data are presented as the means±SDs. Comparisons were performed using two-tailed Student's t tests or one-way ANOVA. Kaplan–Meier curves were analyzed by the log-rank test. A p-value of < 0.05 was considered to indicate statistical significance. All data comes from at least three independently repeated experiments.

Results

Expression of the *SMAP1* gene in clinical samples and HB cell lines. Immunohistochemical staining of the 67 clinical HB tissue samples revealed that the expression of SMAP1 in HB tumor tissue was significantly greater than that in normal liver tissue ($p < 0.05$; Figures 1A, 1B). To investigate the relationship between SMAP1 expression and outcome in the 67 children with HB, a Kaplan-Meier survival analysis was conducted. The event-free survival (EFS) and overall survival (OS) rates of the high-SMAP1 expression group (N=38) were lower than those of the low-expression group (N=29) (Figure 1C). Additionally, compared with the expression in THLE-2 normal human liver immortalized cells, *SMAP1* mRNA expression was significantly upregulated in HB cells (HuH-6 and Hep-G2) ($p < 0.001$; Figure 1D).

Cytological functional experiments of *SMAP1* in HB. To investigate the specific role of SMAP1 in HB, CCK-8 and cell colony formation assays were used to detect the proliferation ability of HuH-6 and HepG-2 cells after *SMAP1* knockdown and overexpression. Compared with the NC group, *SMAP1* knockdown in HuH-6 and HepG-2 cells significantly inhibited tumor cell proliferation (Figures 2A, 2B), whereas SMAP1 overexpression significantly increased tumor cell proliferation ($p < 0.01$; Figures 2C, 2D).

Knockdown of *SMAP1* inhibits subcutaneous xenograft growth in nude mice. To further investigate the effect of SMAP1 on tumor proliferation *in vivo*, stable *SMAP1* knockdown and NC HuH-6 cells were subcutaneously inoculated into nude mice to establish a nude mouse subcutaneous xenograft model. Tumor growth was monitored, and immunohistochemical staining was performed on tumor samples from subcutaneous tumors in nude mice. The protein expression of Ki-67, which is closely related to cell proliferation, and caspase-3, which is closely related to apoptosis, was evaluated in the two groups. Compared with the NC group, *SMAP1* knockdown inhibited subcutaneous xenograft growth in the nude mice (Figures 3A-3H). Compared with that in the NC group, the expression of Ki-67 was significantly lower in the KD group, indicating

inhibition of tumor proliferation ($p < 0.01$). Compared with that in the NC group, the expression of caspase-3 was significantly greater in the KD group, indicating that tumor cell apoptosis occurred ($p < 0.001$; Figures 3I-3K).

SMAP1 regulates C-Kit activation of the ERK/MAPK pathway in HB cells. The effect of *SMAP1* knockdown on the regulatory-related proteins in HuH-6 and HepG2 HB cells was investigated. Western blot analysis revealed that the protein expression levels of C-Kit, p-C-Kit, and p-ERK1/2 were significantly reduced following *SMAP1* knockdown (Figure 4).

***SMAP1* regulates HB proliferation through activation of the ERK/MAPK pathway.** To further clarify whether *SMAP1* participates in HB cell proliferation by regulating the ERK signaling pathway, HuH-6 and HepG2 cells transfected with *SMAP1* overexpression plasmids were treated with the U0126 ERK pathway inhibitor. Changes in the expression of ERK signaling pathway-related proteins were detected by Western blot analysis. The *SMAP1* knockdown-induced reduction of ERK1/2 phosphorylation level was restored by U0126 treatment, while the total ERK1/2 protein level remained unchanged. In addition, the protein expression of p-Rb, a downstream protein regulated by the ERK pathway, was also restored (Figure 5).

HuH-6 and HepG2 cells transfected with a *SMAP1*-targeted small interfering RNA were treated with the C16-PAF ERK pathway agonist. Changes in the expression of ERK signaling pathway-related proteins were detected by Western blot analysis. The *SMAP1* knockdown-induced reduction in the ERK1/2 phosphorylation level was restored by C16-PAF treatment, whereas the total ERK1/2 protein level remained unchanged. The expression of downstream proteins regulated by the ERK pathway, such as c-Myc and p-Rb, was also restored (Figure 6).

SMAP1 activates the ERK/MAPK pathway via C-Kit to regulate HB proliferation. To clarify whether *SMAP1* participates in HB cell proliferation by regulating ERK signaling through C-Kit, HuH-6 and HepG2 cells transfected with the *SMAP1* overexpression plasmid were treated with the ISCK03 C-Kit pathway inhibitor. Changes in the expression of ERK signaling pathway-related proteins were detected by Western blot analysis. Treatment of *SMAP1*-overexpressing cells with ISCK03 increased the C-Kit phosphorylation level and recovered the reduced ERK1/2 phosphorylation level, whereas the total ERK1/2 protein level remained unchanged (Figure 7).

Discussion

HB accounts for 80% of pediatric hepatic malignancies, and its incidence is increasing by 1-2% annually [17]. The etiology of the HB is still unclear, and recurrent and metastatic disease remain the main treatment challenge [18]. The molecular heterogeneity of HB and the scarcity of validated druggable targets have hindered the development of precision therapies. Through whole-exome

sequencing of HB genomes, our previous study identified recurrent copy-number variations encompassing the SMAP1 locus (chr6q13, spanning 11 exons and 194,132 bp) [6]. However, the functional contribution of SMAP1 to HB pathogenesis had not been systematically investigated. The present study demonstrates, for the first time, that SMAP1 is markedly upregulated in HB tissues and cell lines, where it drives tumor proliferation by attenuating C-Kit endocytosis and thereby sustaining ERK1/2 signaling. These findings establish the SMAP1/C-Kit/ERK axis as a novel signaling cascade in HB and nominate SMAP1 as an independent prognostic biomarker and a potential therapeutic target.

The *SMAP1* gene was first identified and reported in 1998 [19]. A previous study has indicated that loss of SMAP1 suppresses the migration of microsatellite-unstable colorectal cancer cells through an Arf6-dependent mechanism, although effects on cell proliferation and C-Kit regulation were not investigated [7]. Another study has reported that deletion of *SMAP1* leads to impaired proliferation of erythroid progenitor cells, but these observations were made in a hematopoietic system with a very limited sample size of less than 10 cases [20]. Based on analyses of 67 HB clinical specimens and two HB cell lines, the present study confirms the involvement of the *SMAP1*-related pathway in a pediatric solid tumor. The application of lentivirus-mediated stable knockdown, pharmacological rescue assays and nude mouse xenograft experiments provides solid causal evidence, with both sample size and depth of functional validation exceeding those of previous studies. A large body of evidence has demonstrated that ligand-activated C-Kit exerts tyrosine kinase activity and initiates downstream signaling cascades that modulate apoptosis, differentiation, proliferation, chemotaxis and cell adhesion, thereby facilitating tumor cell survival and tumorigenesis. A prior investigation has revealed the presence of a TGF-β/C-Kit positive-feedback loop in adult liver cancer, yet the upstream trigger responsible for C-Kit overactivation remains unclear [21]. Using a three-step siRNA-rescue-inhibitor strategy, we demonstrate for the first time that SMAP1 resides upstream of C-Kit and directly regulates its phosphorylation, thus identifying an initiator of C-Kit overactivation. In terms of methodology, we combined exon copy number variation data with high-throughput IHC scoring to construct a *SMAP1* expression prognostic model, and we used lentiviral stable knockdown and transient transfection to provide direct translatable evidence for precise intervention targeting the *SMAP1*/*C-Kit*/ERK axis. The present findings confirmed that the ERK/MAPK pathway is closely linked to HB proliferation. SMAP1 blocks C-Kit endocytosis and enriches it on the membrane, resulting in the hyperphosphorylation of ERK1/2 and the simultaneous activation of

downstream c-Myc and p-Rb; this process can be instantly switched off by U0126, suggesting the synergistic effect of combining MEK inhibitors with SMAP1 silencing. To our knowledge, this is the first report elucidating the role of SMAP1 in HB.

The present study had several limitations. First, although the number of patients in the present study (67 patients) exceed that of most single-center studies, the sample size was modest for a rare disease, and all specimens were obtained from two tertiary hospitals in eastern China; thus, geographic and ethnic homogeneity may limit extrapolation to multiethnic cohorts worldwide. Second, the *in vitro* experiments relied mainly on HuH-6 and Hep-G2 cell lines, both of which harbor TP53 deletion and other specific alterations, which may result in overestimating the prominence of the *SMAP1*/*C-Kit*/ERK axis in other molecular subtypes. Third, the animal model employed subcutaneous xenografts, which lack the native hepatic microenvironment and immune infiltrates, potentially leading to an underestimation of SMAP1-mediated tumor–host interactions. Future efforts will expand along three lines. First, a multicenter, prospective HB registry (≥ 200 cases) will be established, encompassing diverse ethnicities (European, East Asian and Middle Eastern), and uniform CHIC-PRETEXT classification and follow-up protocols will be applied. Whole-exome sequencing and single-cell RNA-seq will be integrated to systematically evaluate *SMAP1* expression across different molecular subtypes and immune microenvironments, validating its stability across populations. Second, Cre-loxP-driven, liver-specific Smap1 conditional-knockout mice and patient-derived xenograft (PDX) models will be generated to compare growth curves, immune infiltration profiles and drug resistance features between subcutaneous and intrahepatic tumors before and after *SMAP1* inhibition, providing a more accurate reflection of the efficacy and therapeutic window of *SMAP1*-targeted strategies. Third, highly selective SMAP1 degraders (PROTACs) or antisense oligonucleotides (ASOs) will be developed, and high-throughput drug screening on organoid-microfluidic chips coupled with real-time imaging and multiparametric metabolic readouts will be performed to rapidly identify synergistic drug pairs (e.g., C-Kit or MEK inhibitors) to provide dosing and biomarker guidance for phase I/II clinical trials. These strategies will compensate for the external validity limitations of the present study and offer a reproducible technical roadmap and evaluation framework for targeting the endocytosis/RTK/MAPK axis in other pediatric solid tumors.

In summary, the present findings revealed for the first time that SMAP1 drives HB proliferation by activating the C-Kit/ERK/MAPK axis and established SMAP1 as an independent prognostic factor

and a novel, druggable target. Verification in multicenter cohorts, orthotopic models and precision combination regimens is needed to further establish SMAP1 as a key component for risk stratification and targeted therapy in HB, laying a solid theoretical and experimental foundation for improving survival outcomes in high-risk children.

Acknowledgments: We thank all the participants and researchers who participated in this study. This study was funded by the Anhui provincial Department of Education university research project (Grant No. 2025AHGXZK20263), the Anhui Provincial Department of Education outstanding young teacher training key project (Grant No. YQZD2023063), New Era Education Quality Project of Anhui Provincial Department of Education (Grant No. 2024zyxwjxalk204), the Wannan Medical University campus level scientific research project (Grant No. WK2022Z06, WK2023ZZD32, WK2023ZQNZ21), the Wannan Medical University Student Research Funding Fund (Grant No. WK2024XS06), the Open Project of Shandong Key Laboratory of Digital Medicine and Computer Assisted Surgery (SDDMKLB-2025-001), the Anhui Province College Students Innovation and Entrepreneurship Training Program Project (Grant No. S202510368059). The funders had no role in the design of the study and collection, analysis, and interpretation of data and in writing the manuscript.

Supplementary data are available in the online version of the paper.

References

[1] PIO L, O'NEILL AF, WOODLEY H, MURPHY AJ, TIAO G et al: Hepatoblastoma. Nat Rev Dis Primers 2025; 11: 36. https://doi.org/10.1038/s41572-025-00620-7

[2] FAN L, NA J, SHI T, LIAO Y. Hepatoblastoma: From Molecular Mechanisms to Therapeutic Strategies. Curr Oncol 2025; 32: 149. https://doi.org/10.3390/curroncol32030149

[3] HIYAMA E, HISHIKI T, YOSHIMURA K, KRAILO M, MAIBACH R et al. Upfront or delayed surgery in resectable hepatoblastoma: analysis from the children's hepatic tumors international collaboration database. E Clinical Medicine 2024; 76: 102811. https://doi.org/10.1016/j.eclinm.2024.102811

[4] CLAVERIA-CABELLO A, HERRANZ JM, LATASA MU, ARECHEDERRA M, URIARTE I et al. Identification and experimental validation of druggable epigenetic targets in hepatoblastoma. J Hepatol 2023; 79: 989-1005. https://doi.org/10.1016/j.jhep.2023.05.031

[5] JIAO J, SAXENA R, MOROTTI R. Hepatoblastoma: Comprehensive Review With Recent Updates. Adv Anat Pathol 2025; 32: 309-316. https://doi.org/10.1097/PAP.0000000000000495

[6] LIU J, GAO C, WANG L, JIAN X, MA M et al. Trans-Ancestry Mutation Landscape of Hepatoblastoma Genomes in Children. Front Oncol 2021; 11: 669560. https://doi.org/10.3389/fonc.2021.669560

[7] SANGAR F, SCHREURS AS, UMANA-DIAZ C, CLAPERON A, DESBOIS-MOUTHON C et al. Involvement of small ArfGAP1 (SMAP1), a novel Arf6-specific GTPase-activating protein, in microsatellite instability oncogenesis. Oncogene 2014; 33: 2758-2767. https://doi.org/10.1038/onc.2013.211

[8] WATANABE A, HATAIDA H, INOUE N, KAMON K, BABA K et al. Arf GTPase-activating proteins SMAP1 and AGFG2 regulate the size of Weibel-Palade bodies and exocytosis of von Willebrand factor. Biol Open 2021; 10: bio058789. https://doi.org/10.1242/bio.058789

[9] HARMS J, LUTTGENAU SM, EMMING C, GUSKE J, WEBER K et al. Pals1 functions in redundancy with SMAP1 to inhibit Arf6 in order to prevent Rac1-dependent colorectal cancer cell migration and invasion. Cancer Gene Ther 2023; 30: 497-506. https://doi.org/10.1038/s41417-022-00570-2

[10] RUHLE F, WITTEN A, BARYSENKA A, HUGE A, ARNING A et al. Rare genetic variants in SMAP1, B3GAT2, and RIMS1 contribute to pediatric venous thromboembolism. Blood 2017; 129: 783-790. https://doi.org/10.1182/blood-2016-07-728840

[11] MIYAUCHI J, KAWAGUCHI H. The in vitro effects of hepatoblastoma cells on the growth and differentiation of blasts in transient abnormal myelopoiesis associated with Down syndrome. Leuk Res 2021; 105: 106570. https://doi.org/10.1016/j.leukres.2021.106570

[12] ZHOU S, ABDIHAMID O, TAN F, ZHOU H, LIU H et al. KIT mutations and expression: current knowledge and new insights for overcoming IM resistance in GIST. Cell Commun Signal 2024; 22: 153. https://doi.org/10.1186/s12964-023-01411-x

[13] LV J, MENG D, ZHANG H, XU W, AN X et al. Apigenin promotes melanogenesis and melanosome transport through the c-KIT/Raf-1/MAPK/CREB pathway in HEMCs. Front Pharmacol 2025; 16: 1572878. https://doi.org/10.3389/fphar.2025.1572878

[14] LIM JM, SUNG HY, PARK SW, HWANG JS. IL-7 secreted by keratinocytes induces melanogenesis via c-kit/MAPK signaling pathway in Melan-a melanocytes. Arch Dermatol Res 2025; 317: 275. https://doi.org/10.1007/s00403-024-03755-x

[15] NAKAJIMA-KOYAMA M, KABATA M, LEE J, SOGABE Y, SAKURAI S et al. The balance between IFN-gamma and ERK/MAPK signaling activities ensures lifelong maintenance of intestinal stem cells. Cell Rep 2025; 44: 115286. https://doi.org/10.1016/j.celrep.2025.115286

[16] LIU J, WU X, XU C, MA M, ZHAO J et al. A Novel Method for Observing Tumor Margin in Hepatoblastoma Based on Microstructure 3D Reconstruction. Fetal Pediatr Pathol 2022; 41: 371-380. https://doi.org/10.1080/15513815.2020.1822965

[17] ZHI T, ZHANG WL, ZHANG Y, HU HM, WANG YZ et al. A new risk-stratification system for hepatoblastoma in children under six years old and the significance for prognosis evaluation-a 14-year retrospective study from a single center. BMC Cancer 2021; 21: 397. https://doi.org/10.1186/s12885-021-08095-x

[18] WU PV, RANGASWAMI A. Current Approaches in Hepatoblastoma-New Biological Insights to Inform Therapy. Curr Oncol Rep 2022; 24: 1209-1218. https://doi.org/10.1007/s11912-022-01230-2
[19] SATO Y, HONG HN, YANAI N, OBINATA M. Involvement of stromal membrane-associated protein (SMAP-1) in erythropoietic microenvironment. J Biochem 1998; 124: 209-216. https://doi.org/10.1093/oxfordjournals.jbchem.a022082
[20] KON S, MINEGISHI N, TANABE K, WATANABE T, FUNAKI T et al. Smap1 deficiency perturbs receptor trafficking and predisposes mice to myelodysplasia. J Clin Invest 2013; 123: 1123-1137. https://doi.org/10.1172/JCI63711
[21] ROJAS A, ZHANG P, WANG Y, FOO WC, MUNOZ NM et al. A Positive TGF-beta/c-KIT Feedback Loop Drives Tumor Progression in Advanced Primary Liver Cancer. Neoplasia 2016; 18: 371-386. https://doi.org/10.1016/j.neo.2016.04.002
[22] LIU J, GAO C, WANG L, JIAN X, MA M et al. Trans-Ancestry Mutation Landscape of Hepatoblastoma Genomes in Children. Front Oncol 2021; 11: 669560. https://doi.org/10.3389/fonc.2021.669560

Figure Legends

Figure 1. SMAP1 protein expression in hepatoblastoma, survival analysis, and screening of small interfering RNA sequences. A, B) IHC analysis of clinical samples revealed that SMAP1 was significantly overexpressed in hepatocellular carcinoma tumor tissue but had low expression in normal liver tissue. Original magnifications, 200×. C) Kaplan-Meier survival analysis of SMAP1 expression in 67 pediatric HB patients. The median IHC score of 5 was used as the cut-off value to define high-SMAP1 (score ≥ 5, n=38) and low-SMAP1 (score < 5, n=29) groups according to our previous study [22]. D) Using actin as an internal reference, qRT-PCR experiments revealed that compared to THLE-2 normal human liver immortalized cells, SMAP1 mRNA expression was significantly upregulated in HB cells (HuH-6 and Hep-G2 cells) ($p < 0.001$). E) Hep-G2 cells were transfected with three small interfering RNA sequences targeting the SMAP1 gene, namely, st-h-SMAP1-1, st-h-SMAP1-2, and st-h-SMAP1-3. qRT-PCR was used to detect the knockdown efficiency of SMAP1. The expression level of SMAP1 mRNA in the interference group was significantly lower than that in the negative control and blank control groups. Among them, the knockdown efficiency of st-h-SMAP1-1 was the highest, and this sequence was used in subsequent experiments.

Figure 2. HuH-6 and Hep-G2 cell viability as detected by the CCK8 assay. A, C) The CCK-8 method was used to detect the proliferation of HuH-6 and Hep-G2 cells after knocking down the

SMAP1 gene. SMAP1 knockdown significantly inhibited the proliferation of HuH-6 and Hep-G2 cells in hepatoblastoma, with the effect being more significant after 72 h. Overexpression of SMAP1 increased tumor cell proliferation of HuH-6 cells and Hep-G2 cells after 24 h and 72 h, respectively. **$p < 0.01$; ***$p < 0.001$. B, D) SMAP1 knockdown significantly reduced the proliferation and colony forming ability of HuH-6 and Hep-G2 cells. Overexpression of SMAP1 significantly increased HuH-6 and Hep-G2 proliferation and colony forming ability. **$p < 0.01$; ***$p < 0.001$

Figure 3. Knockdown of SMAP1 inhibits subcutaneous xenograft growth in nude mice. A, B) *In vivo* imaging images of nude mice carrying tumors on days 14 and 21. C) Nude mice bearing tumors and xenografts. D) Growth rate of nude mouse xenografts. E) Changes in body weight of nude mice. F) Volume comparison of nude mouse xenografts. G) Weight comparison of nude mouse xenografts. H) Comparison of the body weights of nude mice. I) HE staining images (Original magnifications, 200×) and IHC images (Ki-67 and caspase-3) of xenografts in nude mice. Original magnifications, 100×. J, K) The expression of Ki-67 in the KD group was significantly lower than that in the NC group, indicating inhibited tumor proliferation. The expression of caspase-3 in the KD group was significantly higher than that in the NC group, indicating increased tumor cell apoptosis. Original magnifications, 100×. *$p < 0.05$; **$p < 0.01$; ****$p < 0.0001$

Figure 4. Western blot analysis of protein expression levels in SMAP1 knockdown cells. After transfecting HuH-6 and Hep-G2 cells with SMAP1-targeted small interfering RNA, Western blot analysis was used to detect the effects of knocking down SMAP1 on the related proteins and phosphorylation levels in the C-Kit and ERK signaling pathways. SMAP1 knockdown significantly inhibited the total protein and phosphorylation level of C-Kit, as well as the phosphorylation level of ERK1/2 protein, but SMAP1 knockdown had no effect on the expression of total ERK1/2 protein. *$p < 0.05$; **$p < 0.01$; ***$p < 0.001$

Figure 5. Rescue experiment of SMAP1-mediated activation of the ERK/MAPK pathway in HB cells (ERK inhibitor). After transfecting HuH-6 and Hep-G2 cells with SMAP1 overexpression plasmids, they were treated with the U0126 ERK pathway inhibitor. Western blot analysis was used to detect changes in ERK signaling pathway-related proteins. The SMAP1 knockdown-induced

reduction in ERK1/2 phosphorylation level was restored with U0126 treatment, while the total ERK1/2 protein level remained unchanged. The expression of the p-Rb downstream protein regulated by the ERK pathway was also restored. *p < 0.05; **p < 0.01; ***p < 0.001

Figure 6. Rescue experiment of SMAP1-mediated activation of the ERK/MAPK pathway in HB cells (ERK agonist). After HuH-6 and Hep-G2 cells were transfected with the SMAP1-targeted small interfering RNA, they were treated with the C16-PAF ERK pathway agonist. Western blot analysis was used to detect changes in ERK signaling pathway-related proteins. The SMAP1 knockdown-induced reduction in ERK1/2 phosphorylation level was restored by C16-PAF treatment, while the total ERK1/2 protein level remained unchanged. The expression of downstream proteins regulated by the ERK pathway, such as c-myc and p-Rb, was also restored. *p < 0.05; **p < 0.01; ***p < 0.001

Figure 7. SMAP1 mediates the activation of the ERK/MAPK pathway via C-Kit in HB cells. After HuH-6 and Hep-G2 cells were transfected with the SMAP1 overexpression plasmid, the cells were treated with the ISCK03 C-Kit pathway inhibitor. The changes in ERK signaling pathway-related proteins were detected by Western blot analysis. As the phosphorylation level of C-Kit protein increased, the phosphorylation level of ERK1/2 protein was also restored, but the total ERK1/2 protein level remained unchanged. *p < 0.05; **p < 0.01; ***p < 0.001

525 **Table 1.** The sequence of the SMAP1 small interfering RNA.

siRNA	positive-sense strand (5'-3')	antisense strand (5'-3')
si-SMAP1_001	CGAUGGGCUUCCUGGAAUA	UAUUCCAGGAAGCCCAUCG
si-SMAP1_002	GAUACAGUGCAUGCAAGAU	AUCUUGCAUGCACUGUAUC
si-SMAP1_003	CAGAUCAAGCAGUGGAAUU	AAUUCCACUGCUUGAUCUG

526

527

528 **Table 2.** The sequence of the primer.

Gene	Upstream primer sequence	Downstream primer sequence
ACTB	GCGTGACATTAAGGAAGC	CCACGTACACTTCATGTGG
SMAP1	CAGTGACCACGGGAACA	GCAGGTAAGGGATAGAAA

529

Fig. 1 Download full resolution image

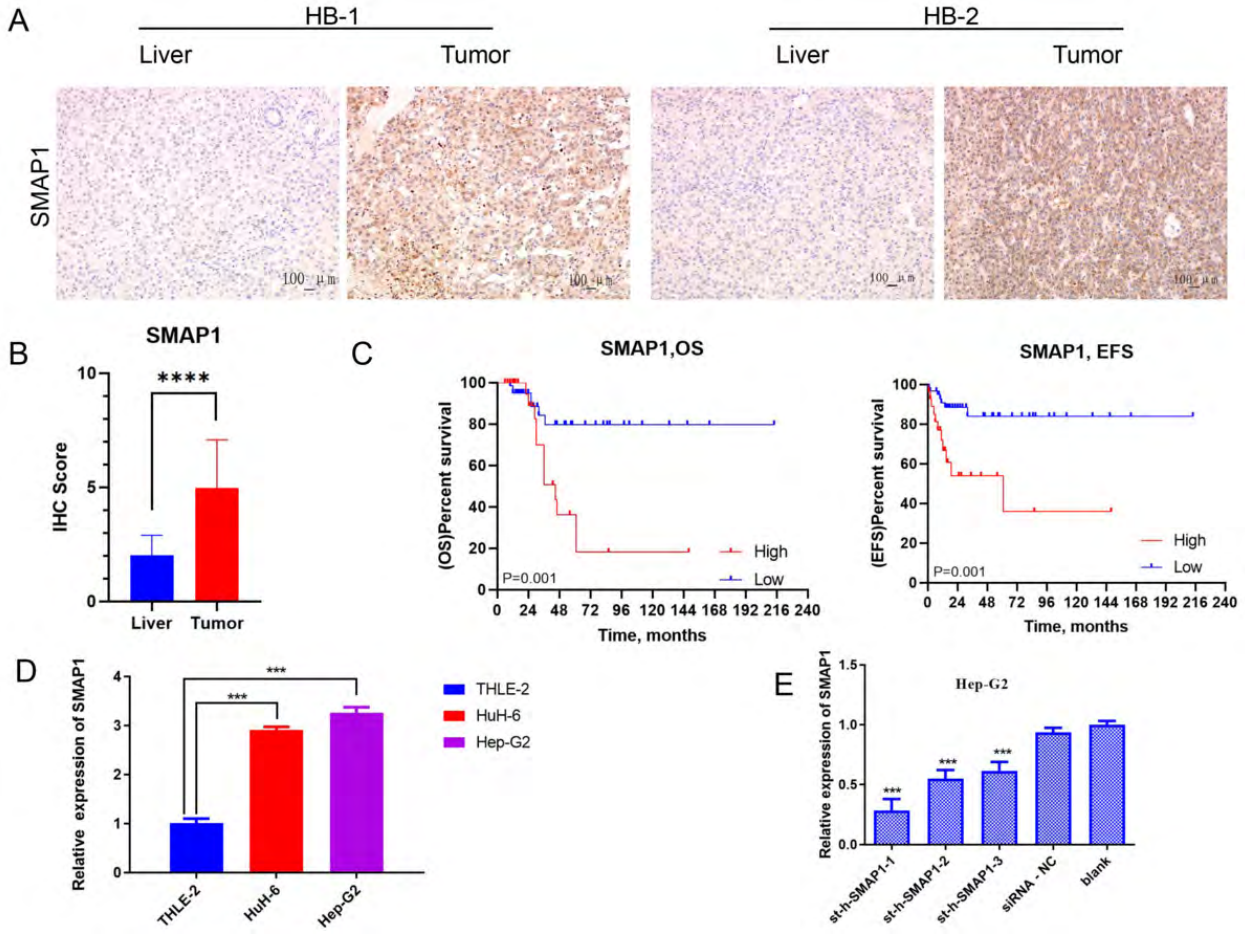

Fig. 2 Download full resolution image

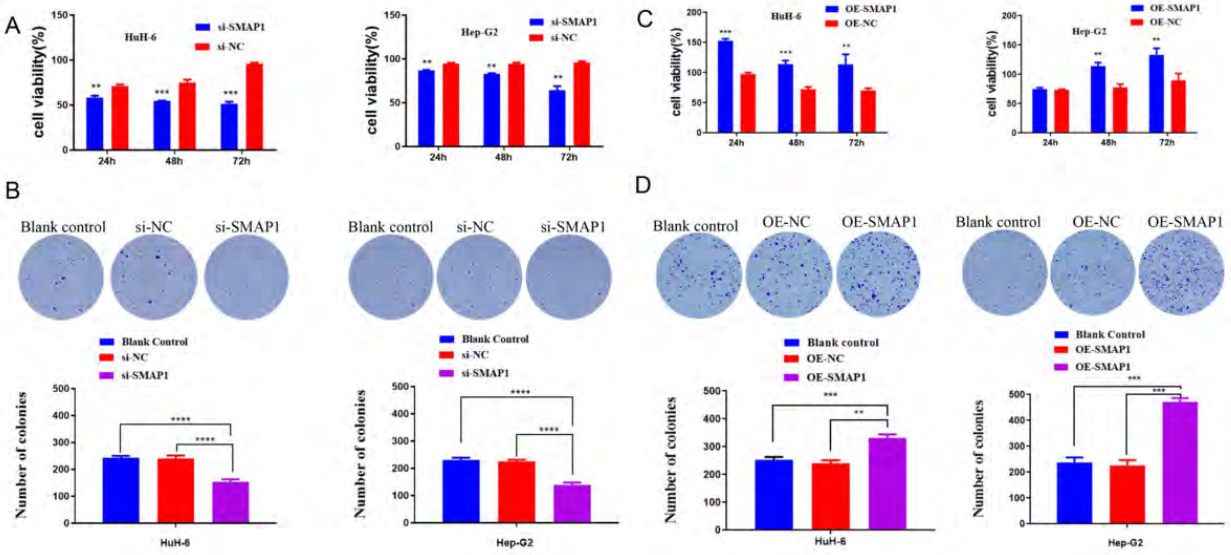

Fig. 3 Download full resolution image

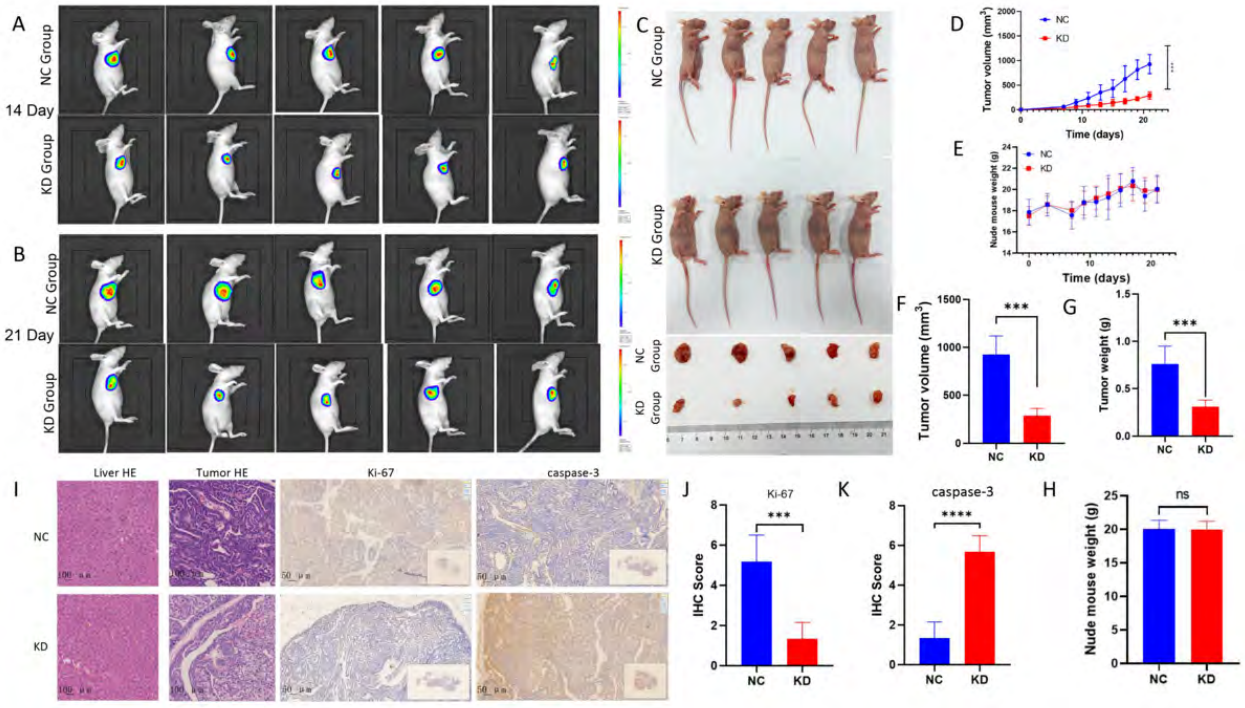

Fig. 4 [Download full resolution image]

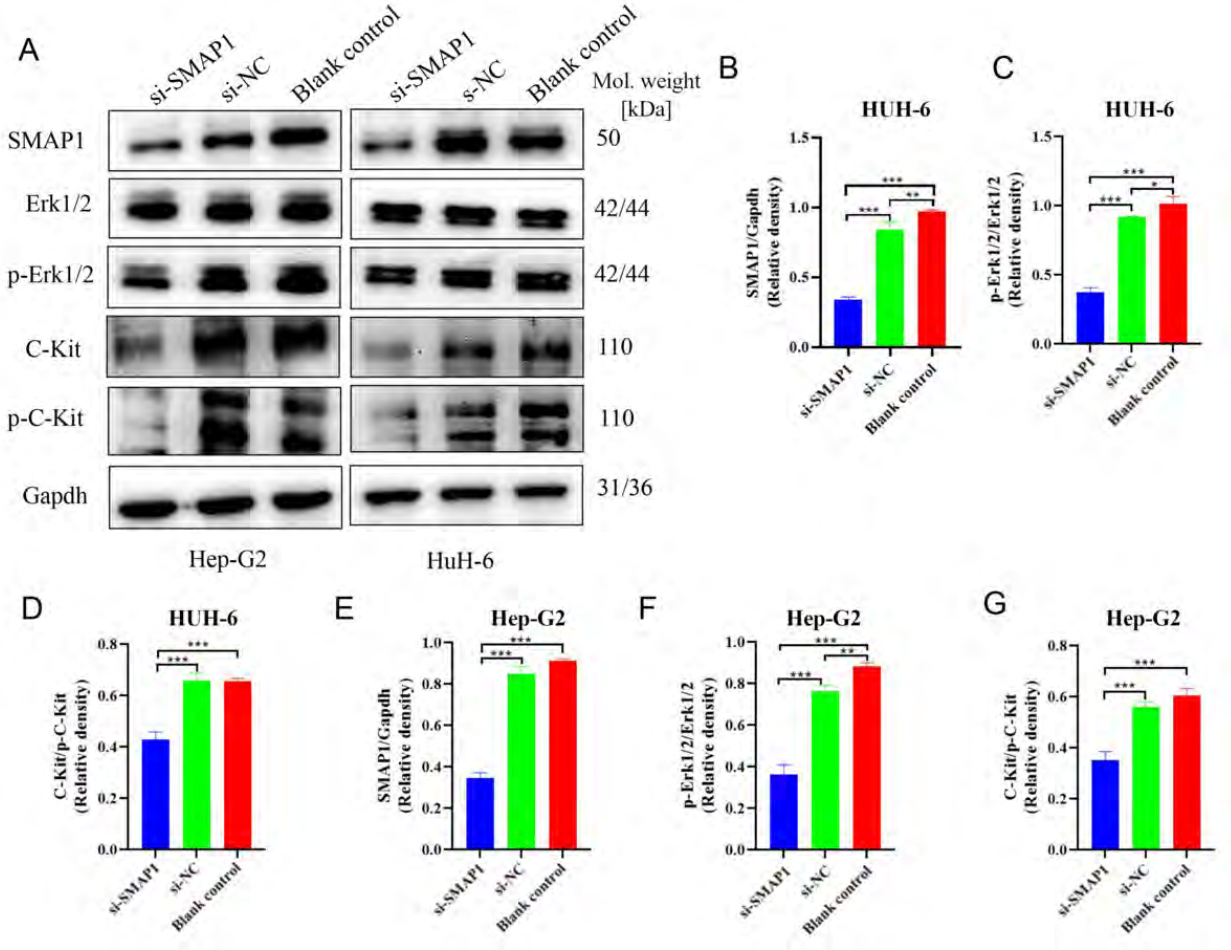

Fig. 5 Download full resolution image

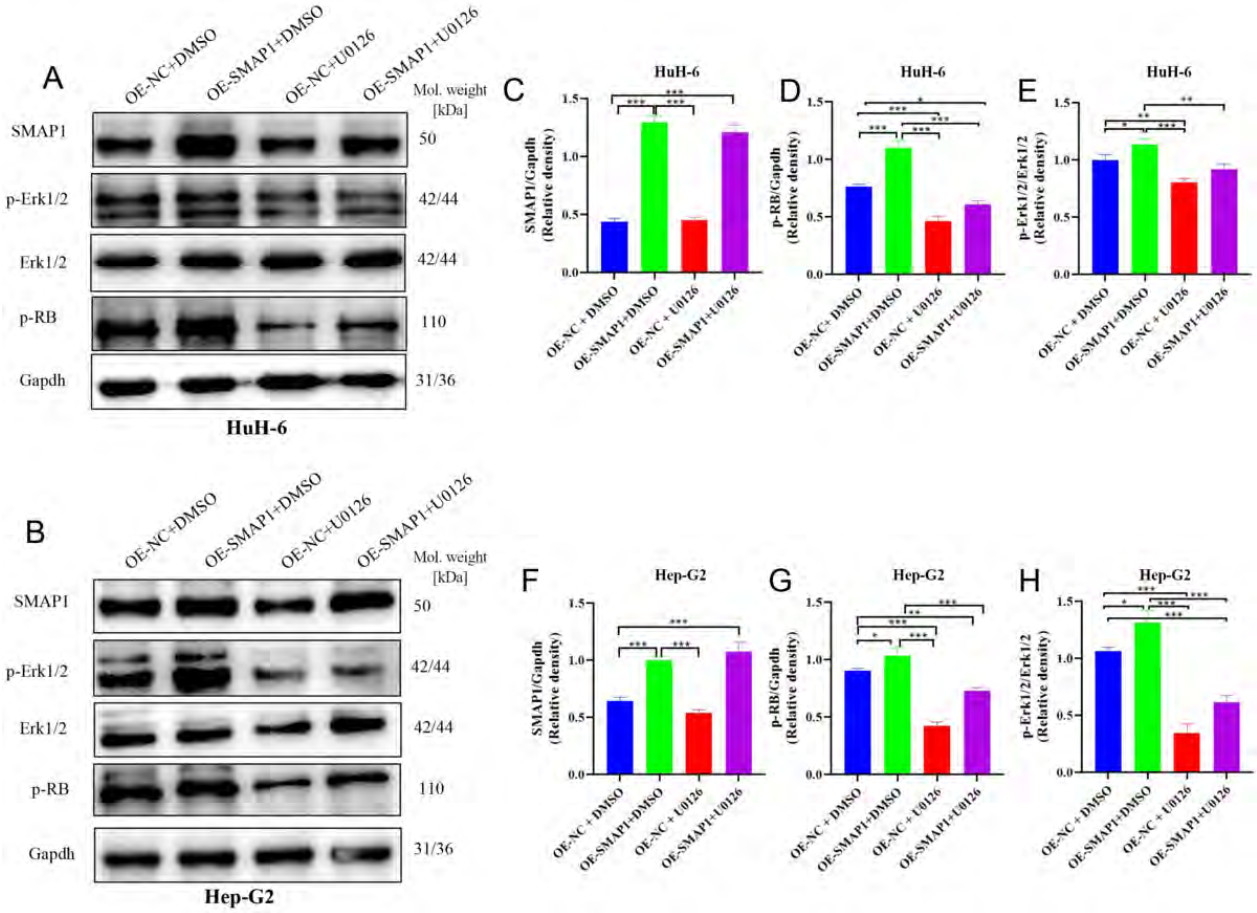

Fig. 6 [Download full resolution image]

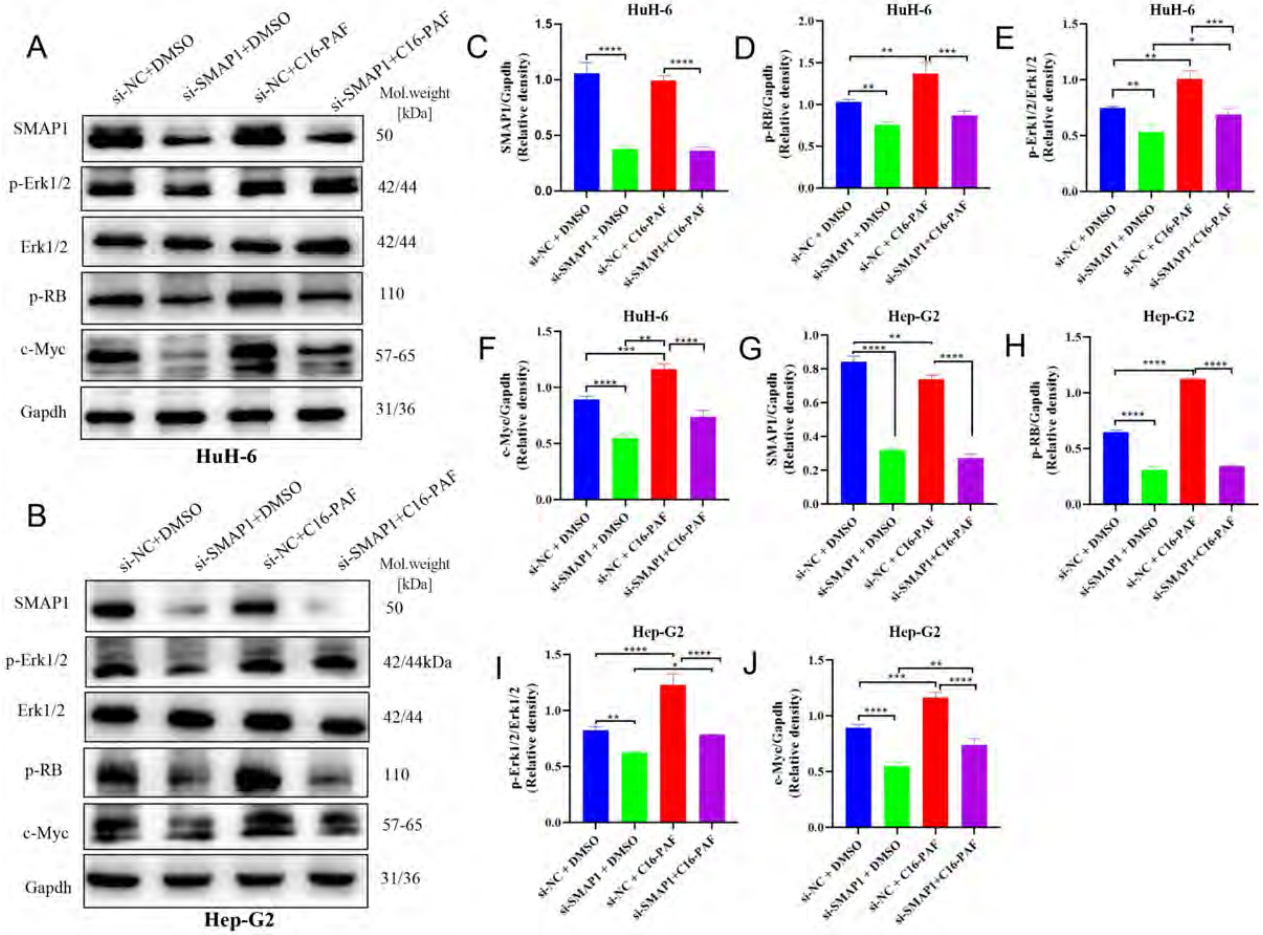

Fig. 7 [Download full resolution image]